Inorg. Chem. **2005**, *44*, 5813–5819

Bivalent and Trivalent Iron Complexes of Acyclic Hexadentate Ligands Providing Pyridyl/Pyrazine–Amide–Thioether Coordination

Akhilesh Kumar Singh and Rabindranath Mukherjee*

Department of Chemistry, Indian Institute of Technology Kanpur, Kanpur 208 016, India

Received January 14, 2005

Acyclic pyridine-2-carboxamide- and thioether-containing hexadentate ligand 1,4-bis[*o*-(pyridine-2-carboxamidophenyl)]-1,4-dithiobutane (H_2bpctb), in its deprotonated form, has afforded purple low-spin ($S = 0$) iron(II) complex [Fe(bpctb)] (**1**). A new ligand, the pyrazine derivative of H_2bpctb, 1,4-bis[*o*-(pyrazine-2-carboxamidophenyl)]-1,4-dithiobutane (H_2bpzctb), has been synthesized which has furnished the isolation of purple iron(II) complex [Fe(bpzctb)]·CH_2Cl_2 (**4**) ($S = 0$). Chemical oxidation of **1** by $[(\eta^5\text{-}C_5H_5)_2Fe][PF_6]$ or $[Ce(NO_3)_6][NH_4]_2$ led to the isolation of low-spin ($S = 1/2$) green Fe(III) complexes [Fe(bpctb)][PF_6] (**2**) or [Fe(bpctb)][NO_3]·H_2O (**3**), and oxidation of **4** by $[Ce(NO_3)_6][NH_4]_2$ afforded [Fe(bpzctb)][NO_3]·H_2O (**5**) ($S = 1/2$). X-ray crystal structures of **1** and **4** revealed that (i) in each case the ligand coordinates in a hexadentate mode and (ii) bpzctb^{2-} binds more strongly than bpctb(2-), affording distorted octahedral $M^{II}N_2$(pyridine/pyrazine)N'_2(amide)S_2(thioether) coordination. To the best of our knowledge, **1** and **4** are the first examples of six-coordinate low-spin Fe(II) complexes of deprotonated pyridine/pyrazine amide ligands having appended thioether functionality. The Fe(III) complexes display rhombic EPR spectra. Each complex exhibits in CH_2Cl_2/MeCN a reversible to quasireversible cyclic voltammetric response, corresponding to the Fe^{III}–Fe^{II} redox process. The $E_{1/2}$ value of **4** is more anodic by ~0.2 V than that of **1**, attesting that compared to pyridine, pyrazine is a better stabilizer of iron(II). Moreover, the $E_{1/2}$ value of **1** is significantly higher (~1.5 V) than that reported for six-coordinate Fe(II)/Fe(III) complexes of the tridentate pyridine-2-carboxamide ligand incorporating thiolate donor site.

Introduction

There has been continued interest in the design of new peptide ligands containing the pyridine-2-carboxamide[1−8] and pyridine-2,6-dicarboxamide[9−11] functionalities to develop their coordination chemistry in the deprotonated form toward Fe(II)/Fe(III). The identification of deprotonated carboxamido N coordination in (i) antitumor drug bleomycins,[12] (ii) iron centers in the P cluster of nitrogenase,[13] and (iii) nitrile hydratases[14] has raised more interest in the area of bioinorganic model studies.[15,16] Some important features of pyridine carboxamide ligands include the good σ-donor properties of

* Author to whom correspondence should be addressed: E-mail: rnm@iitk.ac.in.

(1) Tridentate ligands: (a) Tao, X.; Stephan, D. W.; Mascharak, P. K. *Inorg. Chem.* **1987**, *26*, 754. (b) Noveron, J. C.; Olmstead, M. M. Mascharak, P. K. *Inorg. Chem.* **1998**, *37*, 1138. (c) Tyler, L. A.; Noveron, J. C.; Olmstead, M. M.; Mascharak, P. K. *Inorg. Chem.* **1999**, *38*, 616. (d) Marlin, D. S.; Olmstead, M. M.; Mascharak, P. K. *Eur. J. Inorg. Chem.* **2002**, 859. (e) Rowland, Olmstead, M. M.; Mascharak, P. K. *Inorg. Chem.* **2002**, *41*, 2754.

(2) Tridentate ligands: (a) Wocadlo, S.; Massa, W.; Folgado J.-V. *Inorg. Chim. Acta* **1993**, *207*, 199. (b) Kajiwara, T.; Ito, T. *Acta Crystallogr.* **2000**, *C56*, 22. (c) Kajiwara, T.; Sensui, R.; Noguchi, T.; Kamiyama, A.; Ito, T. *Inorg. Chim. Acta* **2002**, *337*, 299.

(3) Tetradentate ligand: Patra, A. K.; Rose, M. J.; Olmstead, M. M.; Mascharak, P. K. *J. Am. Chem. Soc.* **2004**, *126*, 4780.

(4) Tetradentate ligands: (a) Ray, M.; Mukherjee, R.; Richardson, J. F.; Buchanan, R. M. *J. Chem. Soc., Dalton Trans.* **1993**, 2451. (b) Patra, K.; Mukherjee, R. *Polyhedron* **1999**, *18*, 1317. (c) Patra, A. K.; Ray, M.; Mukherjee, R. *Inorg. Chem.* **2000**, *39*, 652.

(5) Tetradentate ligands: (a) Yang, Y.; Diederich, F.; Valentine, J. S. *J. Am. Chem. Soc.* **1991**, *113*, 7195. (b) Che, C.-M.; Leung, W.-H.; Li, C.-K.; Cheng, H.-Y.; Peng, S.-M. *Inorg. Chim. Acta* **1992**, *196*, 43. (c) Dutta, S. K.; Beckmann, U.; Bill, E.; Weyhermüller, T.; Wieghardt, K. *Inorg. Chem.* **2000**, *39*, 3355.

(6) Bis-tetradentate ligands: Beckmann, U.; Bill, E.; Weyhermüller, T.; Wieghardt, K. *Inorg. Chem.* **2003**, *42*, 1045.

(7) Tetradentate, acting as tridentate: Zhu, S.; Brennessel, W. W.; Harrison, R. G.; Que, L., Jr. *Inorg. Chim. Acta* **2002**, *337*, 32.

(8) Pentadentate ligand: (a) Rowland, J. M.; Olmstead, M. M. Mascharak, P. K. *Inorg. Chem.* **2001**, *40*, 2810. (b) Patra, A. K.; Afshar, R.; Olmstead, M. M.; Mascharak, P. K. *Angew. Chem. Int. Ed.* **2002**, *41*, 2512. (c) Patra, A. K.; Afshar, R. K.; Rowland, J. M.; Olmstead, M. M.; Mascharak, P. K. *Angew. Chem., Int. Ed.* **2003**, *42*, 4517. (d) Patra, A. K.; Rowland, J. M.; Marlin, D. S.; Bill, E.; Olmstead, M. M.; Mascharak, P. K. *Inorg. Chem.* **2003**, *42*, 6812.

(9) Tridentate ligands: Ray, M.; Ghosh, D.; Shirin, Z.; Mukherjee, R. *Inorg. Chem.* **1997**, *36*, 3568.

(10) Pentadentate ligands: (a) Marlin, D. S.; Olmstead, M. M.; Mascharak, P. K. *Inorg. Chim. Acta* **2000**, *297*, 106. (b) Noveron, J. C.; Olmstead, M. M.; Mascharak, P. K. *J. Am. Chem. Soc.* **2001**, *123*, 3247.

10.1021/ic050057s CCC: $30.25
Published on Web 07/12/2005

the coordinated nitrogen, the ability to stabilize metal ions in high oxidation states,[17] and the ease of synthesis of the free ligands. Moreover, the M^{III}−bis(ligand) complexes (M = Fe, Co, Ru) of the tridentate ligand[9,18] and *trans*-{$Fe^{III}(X)_2$} (X = Cl^-, N_3^-, CN^-, PBu_3) complexes of the tetradentate ligand system[4a,c,5b,c,6] are *noninnocent* as they exhibit ligand-centered oxidation processes and in some cases stabilize ligand π-cation radical species to an appreciable extent allowing their isolation in the solid state.[4c,5c,6,18]

Interestingly, the number of Fe(III) complexes with coordinated carboxamido nitrogens is steadily increasing.[16] Quite in contrast, only a few examples are known in which coordination of deprotonated carboxamido nitrogens to Fe(II) centers has been authenticated by X-ray crystallography.[19] However, within this family only one complex is low-spin in character with a pyrimidine-4-carboxamide framework.[20] Thus, no structurally characterized low-spin iron(II) complex with pyridine-2-carboxamide functionality has been reported so far. Clearly, the high σ-donor ability of these carboxamido ligands preclude stabilization of the Fe(II) state with respect to oxidation. To enhance stability we decided to provide thioether (a weak σ-donor-cum-π-acceptor)[21,22] coordination to such Fe(II) environment. Following the observations concerning the coordination behavior of the ligands (i) *N*,*N*′-bis(2′-pyrazinecarboxamido)-1,3-propane (H_2bpzpn)[23] and (ii) *N*,*N*′-bis(2-pyridylmethyl)pyrazine-2,3-dicarboxamide (H_2bpmpz)[24] in the control of molecular architectures and (iii) 1,4-bis[*o*-(pyridine-2-carboxamidophenyl)]-1,4-dithiobutane (H_2bpctb)[25] containing a pyridine−amido−thioether donor set, we have commenced a program to systematically investigate the coordination behavior of (i) $bpctb^{2-}$ and (ii) a new hexadentate ligand 1,4-bis[*o*-(pyrazine-2-carboxamidophenyl)]-1,4-dithiobutane (H_2bpzctb), in its deprotonated form, providing two pyridine/pyrazine N, two amido N, and two thioether S donor sites, toward Fe(II) and Fe(III).

It is worth noting here that the binding properties of thioether sulfur, which has a poor coordinating ability to metal ions in comparison with thiolates, are of interest in coordination chemistry/bioinorganic chemistry.[21,22] However, when it is placed either as a part of strong chelating acyclic ligands or in a macrocyclic environment that binds transition metal ions, a number of such complexes have been synthesized and structurally characterized.[21,22] We wished to investigate (i) the effect of pyrazine N atom (H_2bpzctb) over pyridine (H_2bpctb) in their relative donor potential and metal-centered redox properties, (ii) the strength of M−S(thioether) bonds in the presence of the well-documented deprotonated carboxamide N coordination environment, and (iii) the effect of available electron density on the N atom, not involved in primary coordination, for possible participation in hydrogen-bonding interactions or coordination to other metal ion.

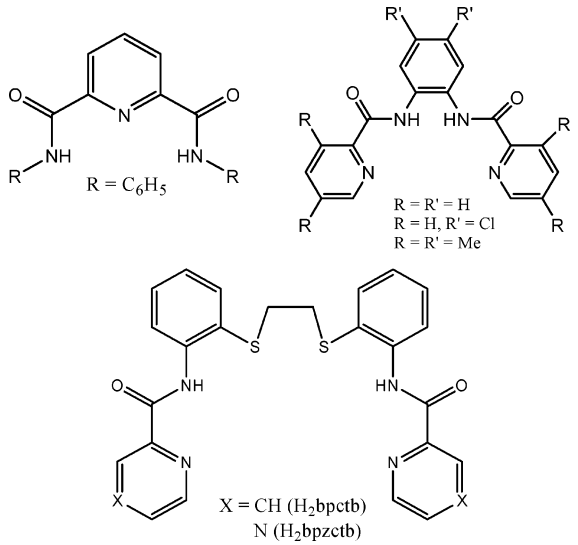

Here, we report the synthesis and characterization (magnetic, spectroscopic, and redox properties) of a family of complexes $[Fe^{II}(bpctb)]$ (**1**), $[Fe^{III}(bpctb)][PF_6]$ (**2**), $[Fe^{III}(bpctb)][NO_3]\cdot H_2O$ (**3**), $[Fe^{II}(bpzctb)]\cdot CH_2Cl_2$ (**4**), and $[Fe^{III}(bpzctb)][NO_3]\cdot H_2O$ (**5**). Structural characterization of **1** and **4** provides the first measure of the Fe^{II}−S(thioether) bond in a deprotonated pyridine/pyrazine amide coordination environment. Furthermore, this work provides an opportunity for comparing the structural and redox properties of Fe(II)/Fe(III) complexes of pseudooctahedral MN_2(pyridine)N'_2(amide)S_2(thioether) coordination with that of the corresponding MN_2(pyridine)N'_2(amide)S_2(thiolate) coordination environment.

Experimental Section

Materials and Reagents. All reagents were obtained from commercial sources and used as received. Solvents were dried/purified as reported previously.[4,9] The diamine, 1,2-bis(2-aminophe-

(11) Pentadentate ligand, acting as tridentate: (a) Marlin, D. S.; Olmstead, M. M.; Mascharak, P. K. *Inorg. Chem.* **1999**, *38*, 3258. (b) Harrop, T. C.; Tyler, L. A.; Olmstead, M. M.; Mascharak, P. K. *Eur. J. Inorg. Chem.* **2003**, 475.
(12) (a) Burger, R. M. *Struct. Bonding (Berlin)* **2000**, *97*, 287. (b) Wolkenberg, S. E.; Boger, D. L. *Chem. Rev.* **2002**, *102*, 2477.
(13) Peters, J. W.; Stowell, M. H.; Soltis, M.; Finnegan, M. G.; Johnson, M. K.; Rees, D. C. *Biochemistry* **1997**, *36*, 1181.
(14) Kobayashi, M.; Shimizu, S. *Curr. Opin. Chem. Biol.* **2000,** *4*, 95.
(15) (a) Mascharak, P. K. *Coord. Chem. Rev.* **2002**, *225*, 201. (b) Harrop, T. C.; Mascharak, P. K. *Acc. Chem. Res.* **2004**, *37*, 253.
(16) Marlin, D. S.; Mascharak, P. K. *Chem. Soc. Rev.* **2000**, *29*, 69.
(17) (a) Cr(V) complex: Che, C.-M.; Ma, J.-X.; Wong, W. T.; Lai, T.-F.; Poon, C.-K. *Inorg. Chem.* **1988**, *27*, 2547. (b) Fe(IV) complex: ref 5c. (c) Ni(III) and Ni(IV) complexes: Patra, A. K.; Mukherjee, R. *Inorg. Chem.* **1999**, *38*, 1388.
(18) Singh, A. K.; Balamurugan, V.; Mukherjee, R. *Inorg. Chem.* **2003**, *42*, 6497.
(19) Examples of structurally characterized Fe(II) complexes of deprotonated pyridinecarboxamide ligands include the following: $[Fe(Prpep)_2]\cdot 2MeOH$ (*S* = 0) (PrpepH = *N*-(2-(4-imidazolyl)ethyl)-pyrimidine-4-carboxamide);[20] $[Fe(bpca)_2]\cdot H_2O$ (*S* = 0 with a residual paramagnetic fraction);[2a] $[Fe(L)_2]$ (*S* = 2) (HL= *N*-(bis(2-pyridyl)-methyl)pyridine-2-carboxamide);[7] $[Et_4N]_2[Fe(PyPS)]$ (*S* = 2) ($PyPSH_4$ = *N*,*N*′-bis(2-mercaptophenyl)pyridine-2,6-dicarboxamide).[10b]
(20) Brown, S. J.; Olmstead, M. M.; Mascharak, P. K. *Inorg. Chem.* **1990**, *29*, 3229.
(21) Blake, A. J.; Schröder, M. *Adv. Inorg. Chem.* **1990**, *35*, 1.
(22) (a) Cooper, S. R. *Acc. Chem. Res.* **1988**, *21*, 141. (b) Cooper, S. R.; Rawle, S. C. *Struct. Bonding (Berlin)* **1990**, *72*, 1.
(23) Challita-Bechara, A.; Chiumia, G. C.; Craig, D. C.; Phillips, D. J.; Rae, A. D. *Inorg. Chim. Acta* **1998**, *271*, 210.
(24) (a) Hausmann, J.; Jameson, G. B.; Brooker, S. *Chem. Commun.* **2003**, 2992. (b) Hausmann, J.; Brooker, S. *Chem. Commun.* **2004**, 1530.
(25) Hexadentate ligand: Sunatsuki, Y.; Matsumoto, T.; Fukushima, Y.; Mimura, M.; Hirohata, M.; Matsumoto, N.; Kai, F. *Polyhedron* **1998**, *17*, 1943.

nylthio)ethane[26] as precursor of thioether functionality, $[Fe(MeCN)_4][ClO_4]_2$,[27] and tetra-*n*-butylammonium perchlorate (TBAP)[28] were prepared by following reported procedures. The ligand 1,4-bis[*o*-(pyridine-2-carboxamidophenyl)]-1,4-dithiobutane (H_2bpctb)[25] and $[(\eta^5\text{-}C_5H_5)_2Fe][PF_6]$[29] were prepared as reported in the literature.

Ligand Synthesis. 1,4-Bis[*o*-(pyrazine-2-carboxamidophenyl)]-1,4-dithiobutane (H_2bpzctb). Pyrazine-2-carboxylic acid (0.90 g, 7.24 mmol) was dissolved in pyridine (5 mL); to the solution a suspension of 1,2-bis((2-aminophenyl)thio)ethane in pyridine (1.0 g, 3.62 mmol in 5 mL) was added dropwise, and the mixture was stirred for 10 min at room temperature. The temperature was slowly then raised to 110 °C. To the reaction mixture triphenyl phosphite (2.24 g, 7.24 mmol) was added dropwise and the mixture was refluxed with stirring for 5 h. It was then cooled and kept in open air. After 12 h, the solid that formed was washed with water several times. Washing with methanol (2 × 10 mL) afforded a white crystalline shiny solid. Yield: 1.25 g (∼80%). Anal. Calcd for $C_{24}H_{18}N_6O_2S_2$: C, 59.26; H, 3.70; N, 17.28. Found: C, 59.42; H, 3.67; N, 17.43. ^{1}H NMR ($CDCl_3$): δ 11.2 (2H, s, NH), 9.53−7.03 [16H, m, aromatic protons (pyridine ring and benzene ring protons)], 3.0 (4H, s, SCH_2).

Synthesis of Metal Complexes. [Fe^{II}(bpctb)] (1). The ligand H_2bpctb (0.5 g, 1.025 mmol) was dissolved in *N*,*N*′-dimethylformamide (DMF) (20 mL), and to it was added solid NaH (0.050 g, 2.05 mmol). The combination was stirred for 15 min resulting in a light yellow solution. To this solution, solid $[Fe(MeCN)_4][ClO_4]_2$ (0.430 g, 1.025 mmol) was added portionwise. The resulting deep purple solution was stirred for 2 h and filtered. The volume of the solution was reduced to ∼5 mL and kept in open air for slow evaporation. After 3−4 days the crystalline purple solid that precipitated was filtered out and dried in air. Recrystallization was achieved by layering of *n*-hexane over CH_2Cl_2 solution of the complex (yield: 0.330 g, ∼60%). Crystals that obtained were found to be suitable for diffraction studies.

Characterization of 1. Anal. Calcd for $C_{26}H_{20}N_4O_2S_2Fe$: C, 57.79; H, 3.70; N, 10.37. Found: C, 57.92; H, 3.67; N, 10.43. Conductivity (DMF, ∼1 mM solution at 298 K): $\Lambda_M = 22\ \Omega^{-1}$ cm^2 mol^{-1} (expected range[30] for 1:1 electrolyte: 65−90 Ω^{-1} cm^2 mol^{-1}). IR (KBr, cm^{-1}, selected peak): 1611 (ν(CO)). Absorption spectrum [λ_{max}, nm (ϵ, M^{-1} cm^{-1})] (in CH_2Cl_2): 250 (42 000), 320 (29 000), 390 sh (7500), 530 (7300).

[Fe^{III}(bpctb)][PF$_6$] (2). To a magnetically stirred solution of **1** (0.100 g, 0.185 mmol) in CH_2Cl_2 (10 mL) was added dropwise a solution of $[(\eta^5\text{-}C_5H_5)_2Fe][PF_6]$ (0.062 g, 0.185 mmol) in CH_2Cl_2 (10 mL). The green microcrystalline compound that precipitated was collected by filtration and washed with CH_2Cl_2. The solid thus obtained was dried in vacuo (yield: 0.102 g, ∼80%).

Characterization of 2. Anal. Calcd for $C_{26}H_{20}N_4O_2S_2PF_6Fe$: C, 45.56; H, 2.90; N, 8.18. Found: C, 45.66; H, 2.72; N, 8.38. Conductivity (MeCN, ∼1 mM solution at 298 K): $\Lambda_M = 130\ \Omega^{-1}$ cm^2 mol^{-1} (expected range[30] for 1:1 electrolyte: 120−160 Ω^{-1} cm^2 mol^{-1}). IR (KBr, cm^{-1}, selected peaks): 840 ($\nu(PF_6^-)$), 1633 (ν(CO)). Absorption spectrum [λ_{max}, nm (ϵ, M^{-1} cm^{-1})] (in MeCN): 240 (23 200), 300 (10 400), 340 sh (5700), 390 (3900), 728 (2260).

[Fe^{III}(bpctb)][NO$_3$]·H$_2$O (3). To a magnetically stirred solution of **1** (0.100 g, 0.182 mmol) in CH_2Cl_2 (10 mL) was added dropwise a solution of $[Ce(NO_3)_6][NH_4]_2$ (0.150 g, 0.273 mmol) in Me_2CO (10 mL). The green microcrystalline solid that precipitated was collected by filtration, washed with diethyl ether, and dried in vacuo (yield: 0.086 g, ∼76%).

Characterization of 3. Anal. Calcd for $C_{26}H_{22}N_5O_6S_2Fe$: C, 50.33; H, 3.55; N, 11.29. Found: C, 49.82; H, 3.61; N, 11.56. Conductivity (MeCN, ∼1 mM solution at 298 K): $\Lambda_M = 127\ \Omega^{-1}$ cm^2 mol^{-1}. IR (KBr, cm^{-1}, selected peaks): 3380 (ν(OH)), 1618 (ν(CO)), 1383 and 837 ($\nu(NO_3^-)$). Absorption spectrum [λ_{max}, nm (ϵ, M^{-1} cm^{-1})]: (in MeCN) 248 (28 150), 300 (12 600), 340 sh (6900), 390 (4560), 725 (2080).

[Fe^{II}(bpzctb)]·CH$_2$Cl$_2$ (4). The ligand H_2bpzctb (0.500 g, 1.025 mmol) was dissolved in DMF (20 mL), and to it was added solid NaH (0.050 g, 2.05 mmol), resulting in a light yellow solution. To it solid $[Fe(MeCN)_4][ClO_4]_2$ (0.430 g, 1.025 mmol) was added pinch by pinch. The resulting deep purple solution was stirred for 2 h. Removal of the solvent was followed by addition of CH_2Cl_2 (15 mL) and filtration. Slow evaporation of this solution afforded a crystalline dark purple solid, which was filtered out and washed with a mixture (5 mL) of MeCN−Et_2O (1:5; v/v). The solid thus collected was air-dried (yield: 0.420 g, ∼65%). Recrystallization was achieved by layering of *n*-hexane over CH_2Cl_2 solution of the complex. Crystals that obtained were found to be suitable for diffraction studies.

Characterization of 4. Anal. Calcd for $C_{25}H_{20}N_6O_2S_2Cl_2Fe$: C, 47.86; H, 3.19; N, 13.40. Found: C, 48.02; H, 3.27; N, 13.32. IR (KBr, cm^{-1}, selected peak): 1609 (ν(CO)). Absorption spectrum [λ_{max}, nm (ϵ, M^{-1} cm^{-1})] (in CH_2Cl_2): 262 (30 700), 300 sh (17 400), 356 (14 200), 440 sh (5300), 490 sh (6100), 550 sh (6400), 650 sh (3000).

[Fe^{III}(bpzctb)][NO$_3$]·H$_2$O (5). To a magnetically stirred solution of **4** (0.100 g, 0.182 mmol) in CH_2Cl_2 (10 mL) was added dropwise a solution of $[Ce(NO_3)_6][NH_4]_2$ (0.122 g, 0.222 mmol) in Me_2CO (10 mL). The green microcrystalline solid that precipitated was collected by filtration, washed with diethyl ether, and dried in vacuo (yield: 0.080 g, ∼70%).

Characterization of 5. Anal. Calcd for $C_{24}H_{20}N_7O_6S_2Fe$: C, 46.31; H, 3.21; N, 15.75. Found: C, 46.22; H, 3.11; N, 15.56. Conductivity (MeCN, ∼1 mM solution at 298 K): $\Lambda_M = 160\ \Omega^{-1}$ cm^2 mol^{-1}. IR (KBr, cm^{-1}, selected peaks): 3411 (ν(OH)), 1638 (ν(CO)), 1383 and 837 ($\nu(NO_3^-)$). Absorption spectrum [λ_{max}, nm (ϵ, M^{-1} cm^{-1})]: (in MeCN) 260 (23 500), 330 sh (8000), 420 sh (2700), 780 (1700).

Physical Measurements. Elemental analyses were obtained using Thermo Quest EA 1110 CHNS-O, Milan, Italy. Conductivity measurements were done with an Elico type CM-82T conductivity bridge (Hyderabad, India). Spectroscopic measurements were made using the following instruments: IR (KBr, 4000−600 cm^{-1}), Bruker Vector 22; electronic, Perkin-Elmer Lambda 2 and Agilent 8453 diode-array spectrophotometer; X-band EPR, Varian 109 C and Bruker EMX 1444 EPR spectrometer (fitted with a quartz dewar for measurements at 77 K or at 120 K, respectively). The EPR spectra were calibrated with diphenylpicrylhydrazyl, DPPH (g = 2.0037).

Magnetic Measurements. Magnetic susceptibility measurements on solid samples of **2** and **5** were done with a locally built Faraday balance equipped with an electromagnet with constant-gradient pole caps (Polytronic Corp., Mumbai, India), Sartorius balance M-25-D/S (Göttingen, Germany), a closed-cycle refrigerator, and a Lake Shore temperature controller (Cryo Industries, Atkinson, NH). All measurements were made at a fixed main field strength of ∼6 kG.

(26) Cannon, R. D.; Chiswell, B.; Venanzi, L. M. *J. Chem. Soc. A* **1967**, 1277.
(27) (a) Sugimoto, H.; Sawyer, D. T. *J. Am. Chem. Soc.* **1985**, *107*, 5712. (b) Richert, S. A.; Tsang, P. K. S.; Sawyer, D. T. *Inorg. Chem.* **1989**, *28*, 2471.
(28) Ray, M.; Mukerjee, S.; Mukherjee, R. *J. Chem. Soc., Dalton Trans.* **1990**, 3635.
(29) Ercolani, C.; Gardini, M.; Pennesi, G.; Rossi, G.; Russo, U. *Inorg. Chem.* **1988**, *27*, 422.
(30) Geary, W. J. *Coord. Chem. Rev.* **1971**, *7*, 81.

Table 1. Data Collection and Structure Refinement Parameters for **[Fe^{II}**(bpctb)] (**1**) and [Fe^{II}(bpzctb)]·CH_2Cl_2 (**4**)

param	**1**	**4**
chem formula	$C_{26}H_{20}FeN_4O_2S_2$	$C_{25}H_{20}Cl_2FeN_6O_2S_2$
fw	540.43	626.85
cryst color, habit	purple, block	purple, block
temp/K	100(2)	100(2)
λ/Å	0.710 73	0.710 73
cryst syst	monoclinic	triclinic
cryst size/ mm × mm × mm	0.2 × 0.2 × 0.2	0.3 × 0.2 × 0.2
space group (No.)	$P2_1/c$ (14)	$P\bar{1}$ (2)
a/Å	10.637(9)	9.508(2)
b/Å	14.088(11)	10.616(6)
c/Å	15.758(13)	13.924(2)
α/deg	90.0	105.88(6)
β/deg	108.318(10)	98.37(7)
γ/deg	90.0	103.35(3)
V/Å^3	2241.7(3)	1282.1(3)
Z	4	2
d_{calcd}/g cm^{-3}	1.601	1.620
μ/mm^{-1}	0.894	0.997
no. reflcns collcd	14618	8344
no. unique reflcns	5527 (R_{int} = 0.0261)	6033 (R_{int} = 0.0214)
no. reflcns used [$I > 2\sigma(I)$]	5045	4657
GOF on F^2	1.152	1.039
final R indices [$I > 2\sigma(I)$]	0.0420 (0.0950)	0.0474 (0.1039)
R indices (all data)	0.0469 (0.0971)	0.0681 (0.1115)

The calibration of the system and details of measurements are already reported in the literature.[4b,c,9]

Solution-state magnetic susceptibilities were obtained by the NMR technique of Evans[31] in CH_2Cl_2 or MeCN with a PMX-60 JEOL (60 MHz) NMR spectrometer. Corrections for underlying diamagnetism were applied with use of appropriate constants.[32]

Electrochemical Measurements. Cyclic voltammetric experiments were performed by using a PAR model 370 electrochemistry system consisting of M-174A polarographic analyzer, M-175 universal programmer, and RE 0074 X-Y recorder. The cell contained a glassy-carbon working electrode (PAR model G0021), a Pt wire auxiliary electrode, and a saturated calomel electrode (SCE) as reference electrode. For constant potential electrolysis experiments a Pt mesh was used as the working electrode. Details of the cell configuration are as described before.[28] The solutions were ~1 mM in complex and 0.1 M in supporting electrolyte, TBAP. Under our experimental conditions, the $E_{1/2}$ values (V) for the couple Fc^+/Fc were 0.40 (MeCN) and 0.49 (CH_2Cl_2) vs SCE.[4c] The measured redox potentials at 298 K were converted to the ferrocenium/ferrocene (Fc^+/Fc) reference.

Crystal Structure Determination. Single crystals of suitable dimensions were used for data collection. Diffraction intensities were collected on a Bruker SMART APEX CCD diffractometer, with graphite-monochromated Mo Kα (λ = 0.710 73 Å) radiation at 100(2) K. The data were corrected for absorption. The structures were solved by SIR 92 expanded by Fourier-difference syntheses and refined with the SHELXL 97 package incorporated in WINGX 1.64 crystallographic collective package.[33] The positions of the hydrogen atoms were calculated by assuming ideal geometries but not refined. All non-hydrogen atoms were refined with anisotropic thermal parameters by full-matrix least-squares procedures on F^2. Pertinent crystallographic parameters are summarized in Table 1.

Results and Discussion

Ligand Design. The hexadentate ligand system used in this work, in the deprotonated form, provides pseudooctahedral MN_2(pyridine/pyrazine)N'_2(amide)S_2(thioether) coordination. Our familiarity[4,9,17c,18,28,34] with pyridyl amide ligands has prompted us, for viable thioether coordination, to employ a combination of pyridine/pyrazine amide functionality and the dithiaalkyl fragment, $-S(CH_2)_2S-$, in a single ligand system.

Synthesis and Characterization. The new ligand H_2-bpzctb was prepared in high yield by treating 2-pyrazinecarboxylic acid with the diamine 1,2-bis((2-aminophenyl)thio)-ethane, as precursor of thioether unit, in the presence of triphenyl phosphite in pyridine. The synthesis of Fe(II) complexes **1** and **4** involved reaction of Na_2bpzctb with [Fe-$(MeCN)_4$][ClO_4]$_2$ in DMF at 298 K. The usual workup afforded dark purple air-stable crystals of [Fe^{II}(bpctb)] (**1**) and [Fe^{II}(bpzctb)]·CH_2Cl_2 (**4**). The syntheses of Fe(III) complexes [Fe^{II}(bpctb)][PF_6] (**2**), [Fe^{III}(bpctb)][NO_3]·H_2O (**3**), and [Fe^{II}(bpzctb)][NO_3]·H_2O (**5**) were achieved by chemical ([(η^5-C_5H_5)$_2$Fe][PF_6] or [Ce(NO_3)$_6$][NH_4]$_2$) oxidation of Fe-(II) complexes **1** and **4**, respectively. For all complexes the absence of ν(N−H) in the IR spectrum confirms that the ligands coordinated in the deprotonated form. Elemental analyses, IR, and solution electrical conductivity data[30] are in agreement with the above formulations. The complexes are soluble in common organic solvents such as CH_2Cl_2, MeCN, and DMF. Structures of Fe(II) complexes have been authenticated by X-ray crystallography (vide infra). Unfortunately, all attempts to grow single crystals of Fe(III) complexes **2**, **3**, and **5** for structural analysis failed so far.

Description of the Structures. [Fe(bpctb)] (1). A perspective view of **1** is shown in Figure 1a, while selected bond distances and angles are collected in Table 2. The iron-(II) center is coordinated to the dianionic hexadentate ligand bpctb^{2-} by two amido and two pyridyl nitrogens and two thioether sulfur atoms. Thus, it affords an FeN_2(pyridine)-N'_2(amide)S_2(thioether) coordination sphere. Appreciable distortions from ideal octahedral geometry are apparent.

The angles between trans atoms at the metal center are N(1)−Fe-S(1) 168.11(6)°, N(2)−Fe-N(3) 175.26(7)°, and N(4)−Fe-S(2) 168.06(6)°. The cis angles span a wide range, 81.72(7)−97.25(5)°. The dimethylene bridge of the five-membered FeS_2C_2 ring has a gauche conformation.

Average Fe−N_{py} (py = pyridine) and Fe−N_{amide} distances are 1.9679(7) and 1.9728(2) Å, respectively. As observed in many structures of pyridine amide ligands,[9,10,17c,18] the Fe−N_{amide} bonds are longer than those of the Fe−N_{py} distances. However, the difference in average bond lengths in **1** is quite small (~0.005 Å). The most noteworthy feature of this structure is that an iron(II) center is coordinated by a deprotonated pyridine amide environment, as examples of such systems are scarce,[19,20] given the remarkable stabilizing

(31) Evans, D. F. *J. Chem. Soc.* **1959**, 2003.
(32) O′Connor, C. J. *Prog. Inorg. Chem.* **1982**, *29*, 203.
(33) Farrugia, L. J. *WINGX version 1.64, An Integrated System of Windows Programs for the Solution, Refinement and Analysis of Single-Crystal X-ray Diffraction Data*; Department of Chemistry, University of Glasgow: Glasgow, U.K., 2003.
(34) (a) Ray, M.; Mukherjee, R. *Polyhedron* **1992**, *22*, 2929. (b) Ray, M.; Mukherjee, R.; Richardson, J. F.; Mashuta, M. S.; Buchanan, R. M. *J. Chem. Soc., Dalton Trans.* **1994**, 965. (c) Patra, A. K.; Ray, M.; Mukherjee, R. *J. Chem. Soc., Dalton Trans.* **1999**, 2461.

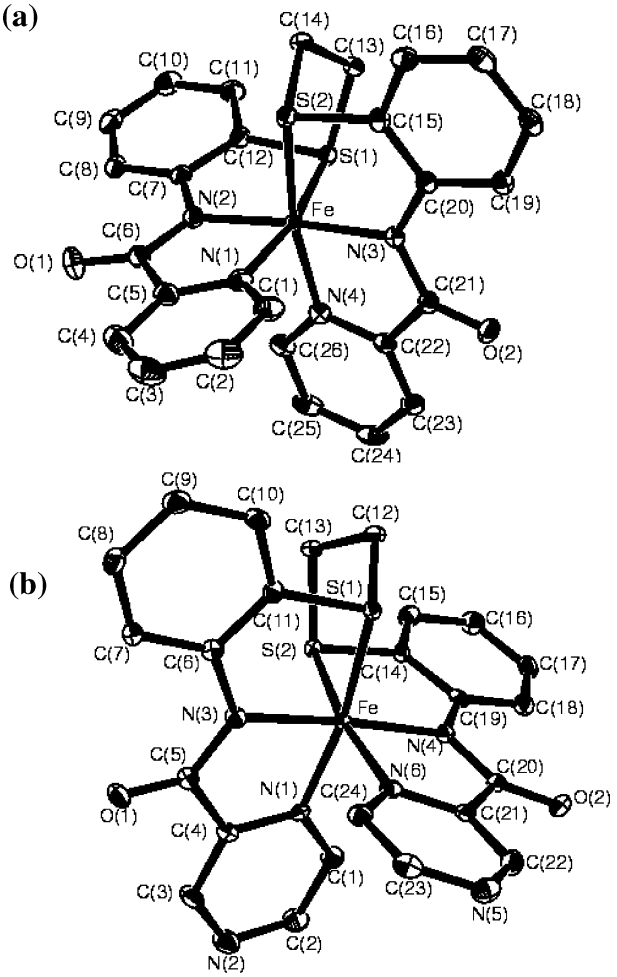

Figure 1. View of the metal coordination environment in the crystals of (a) $[Fe^{II}(bpctb)]$ (**1**) and (b) $[Fe^{II}(bpzctb)]\cdot CH_2Cl_2$ (**4**), showing the atom-labeling scheme and 50% probability ellipsoids. Hydrogen atoms are omitted for the sake of clarity.

power of deprotonated carboxamido nitrogens toward the Fe(III) state.[16] Notably, the average Fe(II) to deprotonated amide nitrogen bond distance is appreciably shorter by ~0.011, ~0.197, and ~0.107 Å than that observed before for octahedral $[Fe(Prpep)_2]\cdot 2MeOH$,[19,20] distorted trigonal bipyramidal $[Et_4N]_2[Fe(PyPS)]$,[10b,19] and octahedral $[Fe(L)_2]$[7,19] Fe(II) complexes, respectively. The average Fe−N_{py} distance is also considerably shorter in **1** [1.9679(7) Å] than that observed for high-spin complexes $[Et_4N]_2[Fe(PyPS)]$[10b,19] [2.129(2) Å] and $[Fe(L)_2]$ [2.187(9) Å].[7,19] However, the data are longer by ~0.013 Å compared to that observed [1.9551 (5) Å] for the Fe−N_{pyrm} (pyrm = pyrimidine) distance observed in the complex $[Fe(Prpep)_2]\cdot 2MeOH$.[19,20] It is interesting to note that average Fe−N_{py} and Fe−N_{amide} distances in **1** are longer by ~0.025 and ~0.049 Å, respectively, than in $[Fe(bpca)_2]\cdot H_2O$.[2a,19]

The two Fe−$S_{thioether}$ lengths in **1** are 2.2478(6) and 2.2558(6) Å. The average Fe^{II}−$S_{thioether}$ length in low-spin $[Fe(9S_3)_2][PF_6]_2$ (9S3 =1,4,7-trithiacyclononane) is 2.250(4) Å.[22b,35] The average length in our low-spin complex is only ~0.005 Å longer. Thus, as a part of the pyridine-2-carboxamide framework, otherwise weakly coordinating thioether S binds the Fe(II) center in **1** quite strongly.

Table 2. Selected Bond Lengths (Å) and Angles (deg) in $[Fe^{II}(bpctb)]$ (**1**) and $[Fe^{II}(bpzctb)]\cdot CH_2Cl_2$ (**4**)

1		**4**	
Fe−N(1)	1.9694(18)	Fe−N(1)	1.931(2)
Fe−N(2)	1.9691(18)	Fe−N(3)	1.965(2)
Fe−N(3)	1.9765(17)	Fe−N(4)	1.965(2)
Fe−N(4)	1.9665(18)	Fe−N(6)	1.945(2)
Fe−S(1)	2.2558(6)	Fe−S(1)	2.2413(8)
Fe−S(2)	2.2478(6)	Fe−S(2)	2.2331(9)
N(1)−Fe−N(2)	81.98(8)	N(1)−Fe−N(3)	82.01(9)
N(1)−Fe−N(3)	94.58(7)	N(1)−Fe−N(4)	94.11(10)
N(1)−Fe−N(4)	91.41(7)	N(1)−Fe−N(6)	90.00(10)
N(1)−Fe−S(1)	168.11(6)	N(1)−Fe−S(1)	169.18(7)
N(1)−Fe−S(2)	90.45(5)	N(1)−Fe−S(2)	91.93(7)
N(2)−Fe−N(3)	175.26(7)	N(3)−Fe−N(4)	175.69(9)
N(2)−Fe−N(4)	95.06(7)	N(3)−Fe−N(6)	95.76(10)
N(2)−Fe−S(1)	86.27(5)	N(3)−Fe−S(1)	87.19(7)
N(2)−Fe−S(2)	96.88(5)	N(3)−Fe−S(2)	95.22(7)
N(3)−Fe−N(4)	81.72(7)	N(4)−Fe−N(6)	82.32(10)
N(3)−Fe−S(1)	97.25(5)	N(4)−Fe−S(1)	96.66(7)
N(3)−Fe−S(2)	86.38(5)	N(4)−Fe−S(2)	86.75(7)
N(4)−Fe−S(1)	91.41(5)	N(6)−Fe−S(1)	90.36(7)
N(4)−Fe−S(2)	168.06(6)	N(6)−Fe−S(2)	169.00(7)
S(1)−Fe−S(2)	89.17(2)	S(1)−Fe−S(2)	89.77(3)

$[Fe(bpzctb)]\cdot CH_2Cl_2$ (4). A view of the metal coordination environment in **4** with the atom numbering scheme is shown in Figure 1b. Selected bond distances and angles are in Table 2. The Fe(II) ion is coordinated by two pyridyl and two amido nitrogen, and two thioether sulfur atoms of this new hexadentate ligand. As in **1**, both the thioether sulfurs are coordinated to Fe(II) and the ligand binds in a hexadentate mode, affording an $FeN_2(pyrazine)N'_2(amide)S_2(thioether)$ coordination sphere. The angles between trans atoms at the metal center are N(1)−Fe-S(1) 169.18(7)°, N(3)−Fe-N(4) 175.69(9)°, and N(6)−Fe-S(2) 169.00(7)°. Similarly, the cis angles span a wide range, 82.01(9)−96.66(7)°. Thus, compared to **1**, distortions from ideal octahedral geometry are slightly less here. As in **1**, the dimethylene bridge has a gauche conformation.

Average Fe−N_{pyrz} (pyrz = pyrazine) and Fe−N_{amide} distances are 1.938(2) and 1.965(2) Å, respectively. In line with the trend observed in **1** (between Fe−N_{py} and Fe−N_{amide} distances), the average Fe−N_{amide} bond length is longer (~0.03 Å) than that of the average Fe−N_{pyrz} distance. Clearly, the difference is more pronounced here. In essence, the structures of **1** and **2** are closely similar; however, a noteworthy difference is that pyrazine N binds the iron(II) center more strongly than pyridine N in a closely similar environment. Compared to **1**, average Fe−N_{amide} and Fe−$S_{thioether}$ distances in **4** are shorter by ~0.008 and ~0.015 Å, respectively.

As observed in **1**, the two Fe−$S_{thioether}$ lengths are dissimilar: 2.2331(8) and 2.2413(8) Å. The average length in this low-spin complex [2.2372(9) Å] is ~0.013 Å shorter than that of the average Fe^{II}−$S_{thioether}$ length in low-spin $[Fe(9S_3)_2][PF_6]_2$ [$9S_3$ = 1,4,7-trithiacyclononane].[22b,35] Thus, as a part of the pyrazine-2-carboxamide framework, thioether S binds the low-spin Fe(II) center in **4** even more strongly than the macrocyclic ligand 9S3. Furthermore, pyrazine-2-

(35) Wieghardt, K.; Küppers, H.-J.; Weiss, J. *Inorg. Chem.* **1985**, *24*, 3067.

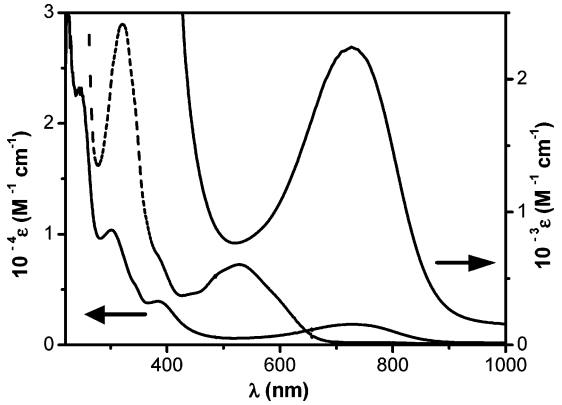

Figure 2. UV−vis spectra of $[Fe^{II}(bpctb)]$ (**1**) in CH_2Cl_2 (dotted line) and $[Fe^{III}(bpctb)][PF_6]$ (**2**) in MeCN (solid line).

carboxamide ligand $bpzctb^{2-}$ provides a better coordinating ability of thioether S than that in the pyridine-2-carboxamide ligand $bpctb^{2-}$. It is interesting to note that thioether S binds Fe(II)/Fe(III) centers strongly giving rise to low-spin complexes when present as part of a strongly chelating ligand.[36]

To the best of our knowledge, **1** and **4** are the first examples of structurally characterized low-spin Fe(II) complexes of a deprotonated pyridine/pyrazine amide ligand incorporating additional thioether coordination.

Absorption Spectra. An intense absorption at 530 nm for **1** and the presence of a series of shoulders in the range 440−550 nm along with a band at 650 nm for **4** justifies their purple color. The green iron(III) complexes **2**, **3**, and **5** are characterized by their charge-transfer transitions in the visible region at 728, 725, and 780 nm, respectively. Representative spectra showing the distinctive features of the complexes are displayed in Figure 2. Spectral signatures of **4** (in CH_2Cl_2) and **5** (in MeCN) are displayed in Figure S1, Supporting Information.[39]

Magnetism and EPR Spectra. Because of the proven strong-field nature of the pyridine carboxamide moiety, which has been shown to afford a low-spin bis-ligand complex of Fe(III) with a tridentate ligand,[9] we wished to investigate the spin-state properties of Fe(II) and Fe(III) complexes of thioether-linked ligands $bpctb^{2-}$ and $bpzctb^{2-}$. The iron(II) complexes **1** and **4** are diamagnetic ($S = 0$). The effective magnetic moment (μ_{eff}) values at 300 K for the iron(III) complexes **2**, **3**, and **5** in the solid state are 2.22, 2.22, and 2.24 μ_B, respectively. The values in MeCN solution for **2** and **5** are 2.13 and 2.17 μ_B, respectively. Thus, solid-state structures are retained in solution. This result corresponds to, for all Fe(III) complexes, an $S = 1/2$ state with an appreciable orbital contribution.[9,37]

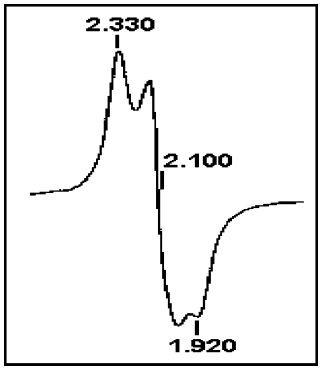

Figure 3. EPR spectrum of a polycrystalline sample of $[Fe^{III}(bpzctb)][NO_3]\cdot H_2O$ (**5**) at 120 K.

As structural information for Fe(III) complexes **3**−**5** is lacking, variable-temperature (81−300 K) measurements on solid samples of **3** and **5** (Figure S2, Supporting Information) were performed to define spin-state and allow structural inferences. As the temperature is lowered, the moment decreases toward the spin-only value, as expected (μ_{eff} values at 81 K were 1.75 and 1.76 μ_B, respectively). The solid-state result implies that the coordination sphere about the iron(III) center in **3** and **5** is distorted octahedral. Given the physicochemical properties of **3**−**5**, it is reasonable to assume that these Fe(III) complexes are uniformly low-spin.

The EPR spectrum of **2** in the solid state at 120 K is not well resolved ($g_{iso} = 2.050$). However, solid samples of **3** displayed at 77 K the rhombic pattern $g_1 = 2.467$, $g_2 = 2.110$, and $g_3 = 1.850$ (Figure S3, Supporting Information). The difference in asymmetry with change in counterion could be due to the crystal packing effect. The spectrum of **5** is displayed in Figure 3. The EPR parameters of these Fe(III) complexes are all close to the g values of other low-spin complexes with deprotonated carboxamido N coordination.[1b,d,4a,c] The observed spectral features must be due to the low symmetry of the $Fe^{III}N_2$(pyridine/pyrazine)N'_2(amide)-S_2(thioether) coordination sphere (cf. X-ray structures of **1** and **4**).

Metal-Centered Redox Activity. To investigate the extent of stabilization of the Fe(II)/Fe(III) state toward oxidation/reduction, cyclic voltammetric (CV) studies were performed.

Fe^{III}−Fe^{II} Couple. In CH_2Cl_2 solution **1** displays a quasireversible[38] Fe^{III}−Fe^{II} redox response at $E_{1/2} = -0.13$ V vs Fc^+/Fc (Figure 4). The one-electron nature of the redox process is revealed by constant potential (0.6 V vs SCE) electrolysis in CH_2Cl_2. The electrogenerated green Fe(III) solutions are stable enough for their CV, absorption, and EPR spectra to be recorded.[39] It is, therefore, logical to assume that there is no gross structural change upon metal redox process. Complex **2** displays in MeCN solution a reversible ($\Delta E_p = 80$ mV)[38] CV response at $E_{1/2} = -0.18$ V vs Fc^+/Fc.

It is worth noting here that in DMF the $E_{1/2}$ value for the Fe^{III}−Fe^{II} couple of Mascharak's complex $[Et_4N][Fe(PyPepS)_2]$ (H_2PyPep = *N*-2-mercaptophenyl-2-pyridinecarboxamide, having FeN_2(pyridine)N'_2(amide)S_2(thiophenolate) coordination,[1b,15b] is more cathodic by 1.48 V than that observed here for **1** having FeN_2(pyridine)N'_2(amide)S_2(thioether) coordina-

(36) Thioether−oxime−azo ligands: Karmakar, S.; Choudhury, S. B.; Chakravorty, A. *Inorg. Chem.* **1994**, *33*, 6148.
(37) Martin, L. L.; Martin, R. L.; Murray, K. S.; Sargeson, A. M. *Inorg. Chem.* **1990**, *29*, 1387.
(38) Under our experimental conditions, the reversible couple Fc^+/Fc in MeCN has a $\Delta E_p = 80$ mV, which was used as the criterion for electrochemical reversibility: Gupta, N.; Mukerjee, S.; Mahapatra, S.; Ray, M.; Mukherjee, R. *Inorg. Chem.* **1992**, *31*, 139.
(39) Absorption spectrum of coulometrically generated $Fe^{III}(bpctb)]^+$ species [λ_{max}, nm (ϵ, M^{-1} cm^{-1})] (in CH_2Cl_2): 246 (22 700), 300 (10 500), 340 sh (5600), 390 sh (3600), 730 (2300). EPR spectrum (CH_2Cl_2, 120 K): $g_1 = 2.376$, $g_2 = 2.137$, $g_3 = 1.946$.

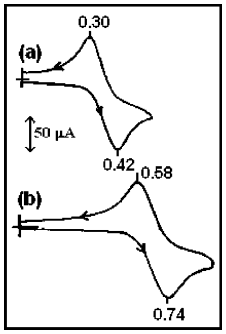

Figure 4. Cyclic voltammograms (100 mV/s) of ~1 mM solution of (a) [Fe^{II}(bpctb)] (**1**) and (b) [Fe^{II}(bpzctb)]·CH_2Cl_2 (**4**) at a glassy carbon electrode in CH_2Cl_2 (~0.1 M in TBAP). Indicated potentials (in V) are vs SCE.

tion. As thiophenolato sulfur is known to stabilize the Fe(III) state over Fe(II) and thioether is a weak σ-donor/π-acceptor ligand, the observed trend is understandable.[40]

In CH_2Cl_2 solution complex **4** displays a quasireversible[38] CV response at $E_{1/2} = 0.17$ V vs Fc^+/Fc, corresponding to the $Fe^{III}-Fe^{II}$ redox process (Figure 4). Thus, in the order from pyridine to pyrazine amide functionality, the iron(II) state is better stabilized by 300 mV, with respect to oxidation, implying a better π-accepting property of pyrazine than pyridine in the Fe(II) state (cf. complexes **1** and **4**) and/or coordinative interaction (the complexes being the donor and the solvent the acceptor; an increase in effective positive charge on the Fe(II) complex would make oxidation difficult).[41] Isolated Fe(III) complex **5** displays in MeCN solution a reversible ($\Delta E_p = 80$ mV)[38] CV response at $E_{1/2} = 0.02$ V vs Fc^+/Fc. It is, therefore, reasonable to assume that **4** and **5** have similar coordination environments.

Solvent Dependency of the $Fe^{III}-Fe^{II}$ Redox Processes. Due to the ready solubility of Fe(II) complexes (**1** and **4**) in CH_2Cl_2 and Fe(III) complexes (**2** and **5**) in MeCN, the present complexes provide a unique opportunity to investigate the effect of solvent on the metal-centered redox thermodynamics. It is worth noting that the free energy of solvation depends[42] on the radius of the ions, the relative permittivity (the dielectric constant) of the solvent, and the possibility of specific bonding (especially hydrogen bonding) between the ions and the solvent. In the order from CH_2Cl_2 to MeCN (dielectric constants: CH_2Cl_2, 8.9; MeCN, 37.5),[42] an appreciable cathodic shift (140 mV between **1** and **2**; 240 mV between **4** and **5**) in the $E_{1/2}$ values is observed. In fact, incremental addition of MeCN to CH_2Cl_2 solutions of **1**/**4** allows one to monitor monotonic decrease (130 mV for **1** and 220 mV for **4**) in $E_{1/2}$ values (complex **1**, Figure S4, Supporting Information; complex **4**, Figure S5, Supporting Information). Notably, for the $Fe^{III}-Fe^{II}$ couple of [Fe^{III}-(tridentate ligand)$_2$]$^-$ the shift of $E_{1/2}$ values (solvents chosen: MeCN, DMF, DMSO, and water) was more dramatic.[9] The present investigation reveals that the Fe(II) state of the complexes **1** and **4** is systematically better stabilized, as the dielectric constant of the medium is decreased. A less dielectric medium is expected to stabilize the neutral form of the Fe(II) complex, as expected.

Acknowledgment. This work is supported by grants from the Council of Scientific and Industrial Research and Department of Science and Technology, Government of India, New Delhi. A.K.S. gratefully acknowledges the award of a fellowship (SRF) by CSIR, Delhi.

Supporting Information Available: Absorption spectra of **4** and **5** (Figure S1), plots of molar susceptibility vs temperature for **3** and **5** (Figure S2), an EPR spectrum of **3** at 77 K (Figure S3), CV scans due to addition of MeCN to CH_2Cl_2 solutions of **1** (Figure S4) and **4** (Figure S5), and crystallographic data in CIF format. This material is available free of charge via the Internet at http://pubs.acs.org.

IC050057S

(40) It should be kept in mind, however, that in addition to difference in solvent there is difference in charge as well during the redox processes. For Mascharak's complex it is 2−/1−, and for the present complexes it is 1+/0.

(41) (a) Gutmann, V.; Gritzner, G.; Danksagmüller, K. *Inorg. Chim. Acta* **1976**, *17*, 81. (b) Mascharak, P. K. *Inorg. Chem.* **1986**, *25*, 245.

(42) Sawyer, D. T.; Roberts, J. L., Jr. *Experimental Electrochemistry for Chemists*; Wiley: New York, 1974; pp 186, 204−207.